Figures and figure supplements

Methylglyoxal-derived hydroimidazolone, MG-H1, increases food intake by altering tyramine signaling via the GATA transcription factor ELT-3 in *Caenorhabditis elegans*

Muniesh Muthaiyan Shanmugam *et al*.

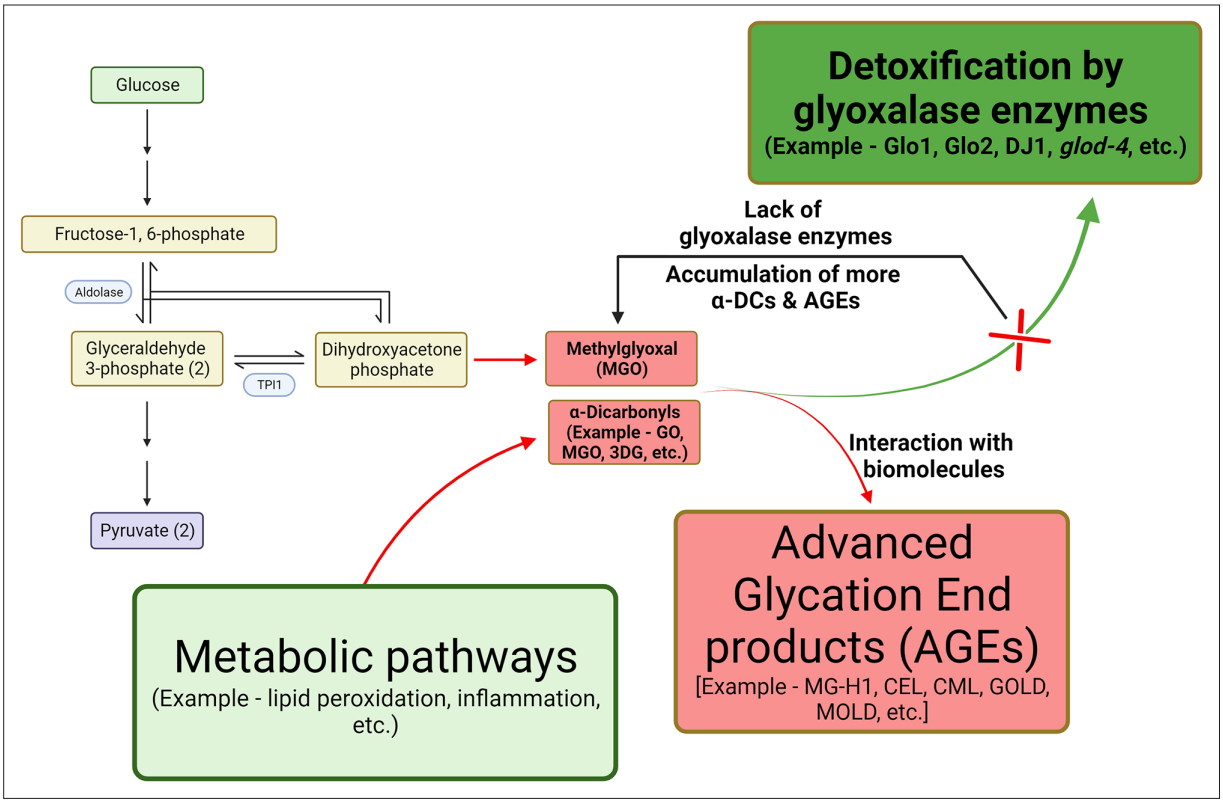

Figure 1. Graphical representation for the formation of α-dicarbonyls and advanced glycation end-products (AGEs). Dicarbonyls are highly reactive byproducts from metabolic pathways such as lipid peroxidation and glycolysis. In the above example, methylglyoxal (MGO) spontaneously forms from dihydroxyacetone phosphate which interacts with biomolecules resulting in the formation of AGEs. Toxic MGO is detoxified by glyoxalase enzymes to non-toxic lactate. One of the examples of glyoxalase enzyme in *C. elegans* is *glod-4*. Lack of glyoxalase enzyme leads to increased levels of MGO resulting in increased accumulation of AGEs.

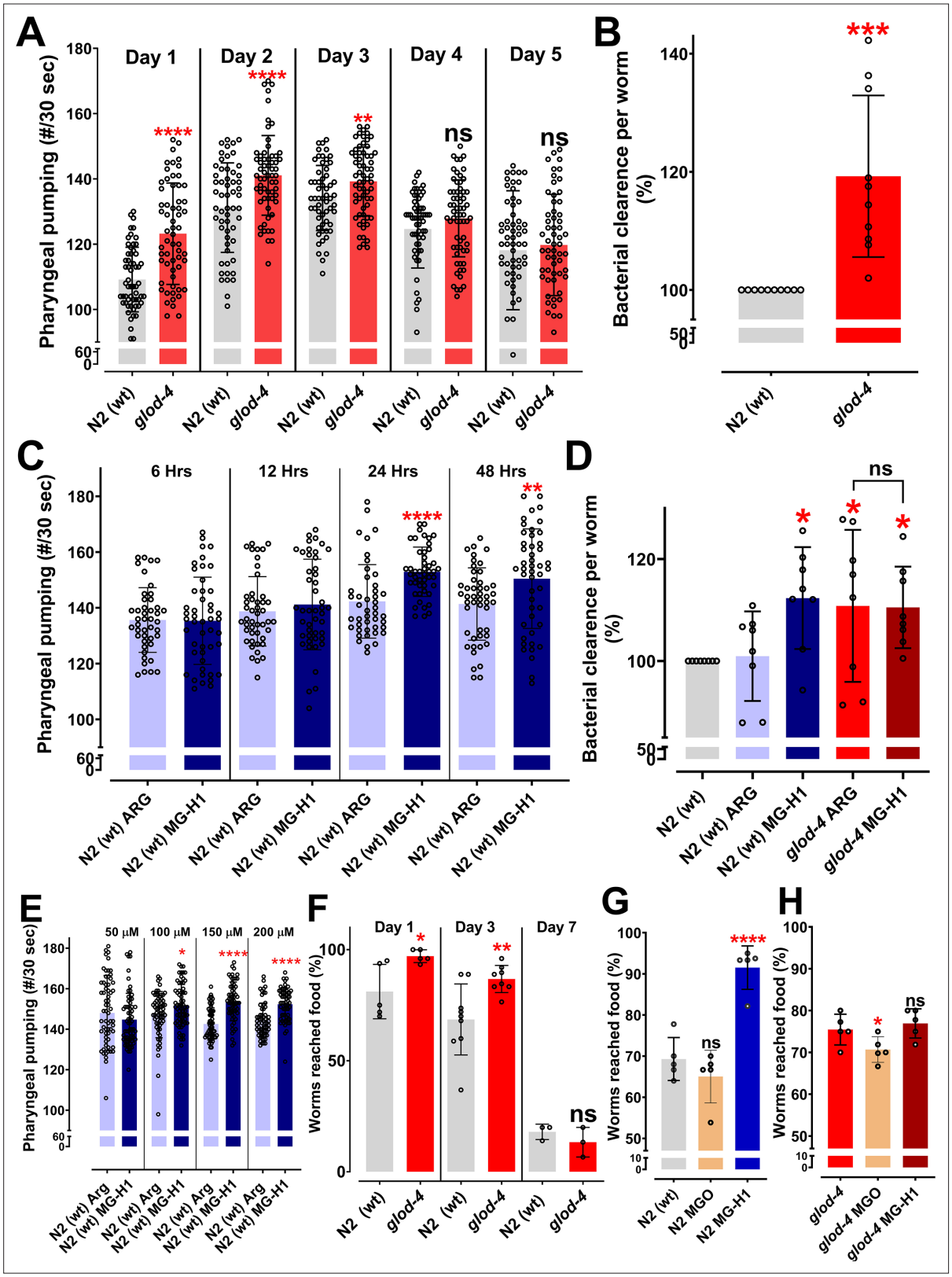

Figure 2. The glyoxalase mutant, *glod-4*, and methylglyoxal (MGO)-derived advanced glycation end-product (AGE), MG-H1, increases pharyngeal pumping and feeding in *C. elegans*. (**A**) Quantification of pharyngeal pumping (#/30 s) in N2 (wt) and *glod-4 (gk189)* mutant at different stages of adulthood. (**B**) Food clearance assay in N2 (wt) and *glod-4 (gk189)* mutant after 72 hr of feeding. (**C**) Quantification of pharyngeal pumping (#/30 s) in N2 (wt) after treatment, with either 150 µM of arginine (control) or MG-H1. (**D**) Food clearance assay in N2 (wt) and *glod-4 (gk189)* mutant worms after

Figure 2 continued on next page

Figure 2 continued

treatment for 72 hr with either 150 μM of arginine (control) or MG-H1. (**E**) Quantification of pharyngeal pumping with different concentrations of MG-H1. (**F**) Food racing assay in N2 (wt) and *glod-4 (gk189)* at different stages of adulthood toward OP50-1. (**G**) Food racing assay of N2 (wt) toward OP50-1 when combined with either MGO or MG-H1 (100 μM). (**H**) Food racing assay of *glod-4 (gk189)* mutants toward OP50-1 when combined with either MGO or MG-H1 (100 μM). Student's *t*-test for A, B, C, E, and F. One-way analysis of variance (ANOVA) with Fisher's LSD (Least Significant Difference) multiple comparison test for D, G, and H. The data points in the graphs represent the sample size (n). Comparison between two specific groups are indicated by lines above the bars; otherwise, the groups are compared with control group. *$p < 0.05$, **$p < 0.01$, ***$p < 0.001$, and ****$p < 0.0001$. Error bar ± standard deviation (SD).

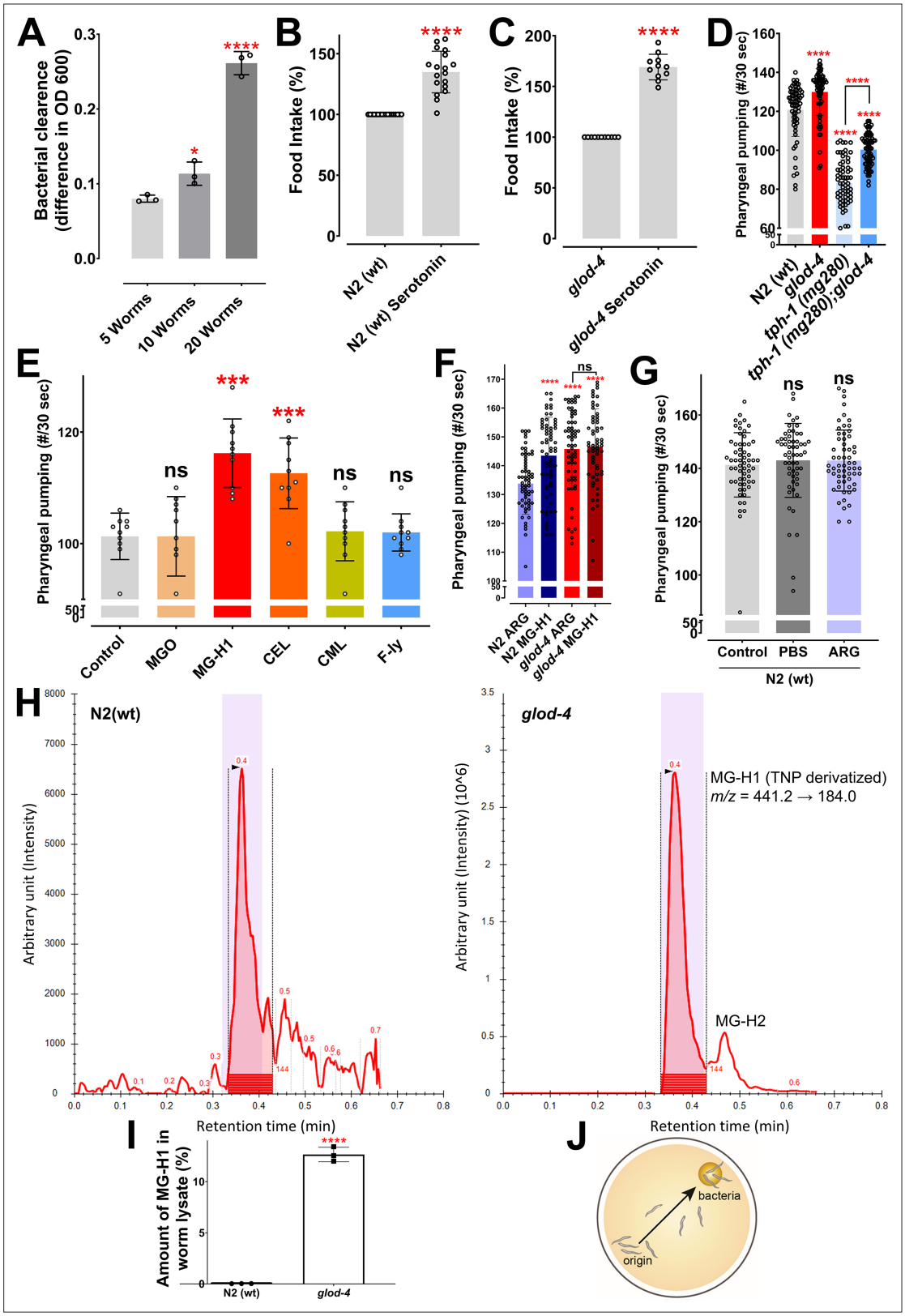

Figure 2—figure supplement 1. The glyoxalase mutant, *glod-4*, and methylglyoxal (MGO)-derived advanced glycation end-product (AGE), MG-H1, increases pharyngeal pumping and feeding in *C. elegans*. (**A**) Food clearance assay demonstrating increased food intake with an increasing number of worms. (**B**, **C**) Food clearance assay of wildtype N2 (wt) and *glod-4 (gk189)* mutant with 5 mM treatment of serotonin, respectively. (**D**) Quantification of pharyngeal pumping in genetic mutants such as *tph-1* (tryptophan hydroxylase), *glod-4*, and *tph-1;glod-4* double mutant compared with N2 (wt)

Figure 2—figure supplement 1 continued on next page

Figure 2—figure supplement 1 continued

wildtype worms. (**E**) Quick visual quantification of pharyngeal pumping after treatment with different advanced glycation end-products (AGEs) molecules at 100 µM for 12–18 hr. (**F**) Quantification of pharyngeal pumping with treatment of either N2 (wt) wildtype or *glod-4* mutants with either arginine or MG-H1 at 150 µM. (**G**) Quantification of pharyngeal pumping in N2 (wt) worms after treatment with phosphate-buffered saline or 150 µM of arginine for 24 hr. (**H**) Liquid chromatography–multiple reaction monitoring (LC-MRM) chromatograms for the exacted ion peaks for TNP-MG-H1 in N2 wildtype (left) and *glod-4* mutant (right). (**I**) Relative quantification of MG-H1 in worm lysates of N2 wildtype and *glod-4* mutant background from (**H**). (**J**) Pictorial representation of food racing assay. Student's *t*-test for B, C, I. One-way analysis of variance (ANOVA) for A, D, E–G. The data points in the graphs represent the sample size (n). *p < 0.05, ***p < 0.001, and ****p < 0.0001. Error bar ± standard deviation (SD).

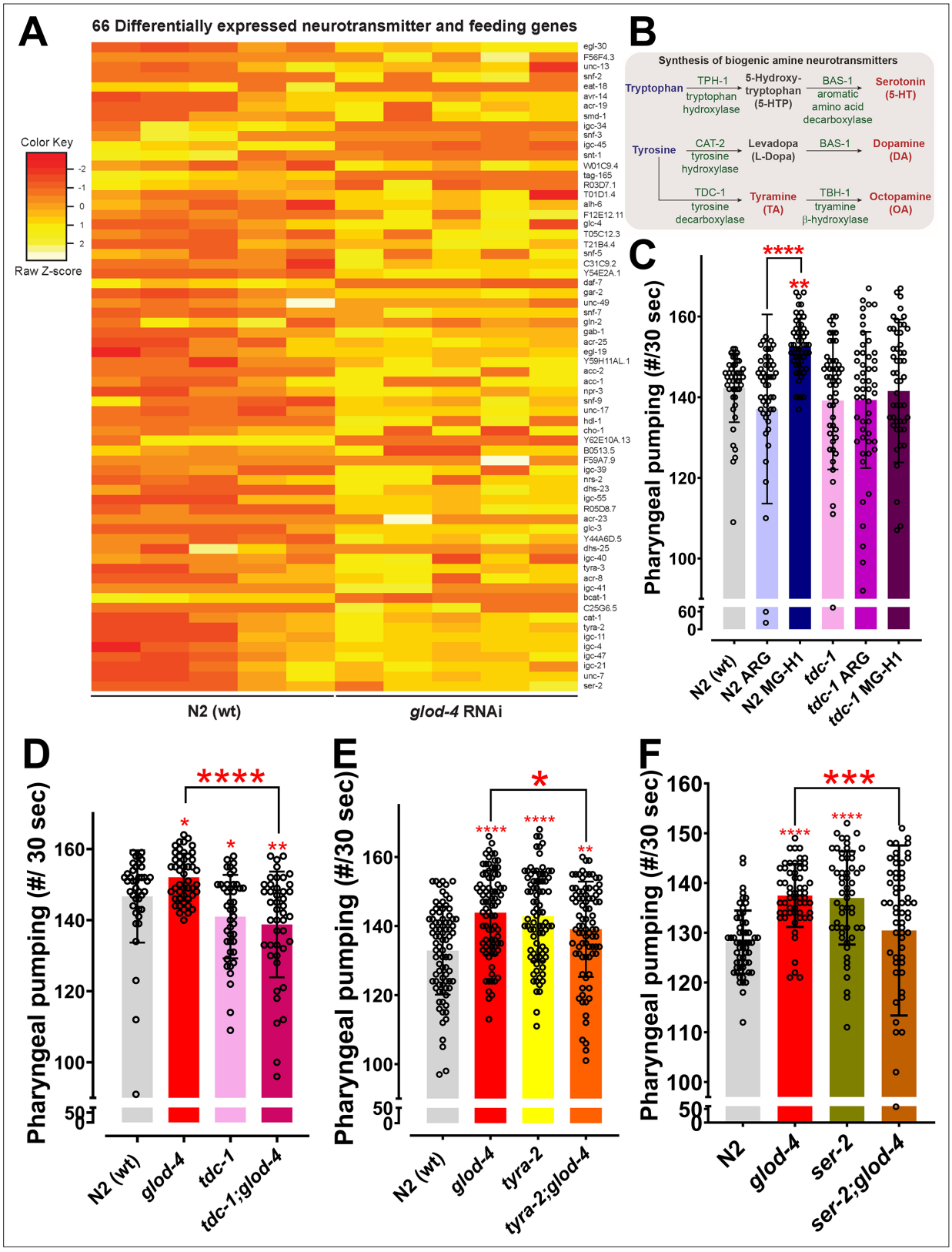

Figure 3. Role of *tdc-1* and tyramine receptors in mediating the MG-H1-induced feeding behavior. (**A**) Differential expression of 66 neurotransmitters and feeding genes in *glod-4* RNAi background. (**B**) The flowchart shows the pathway of biogenic amine synthesis, which functions as a neurotransmitter. (**C**) Quantification of pharyngeal pumping in N2 (wt) and *tdc-1 (n3419)* mutant worms after 24 hr of treatment of MG-H1. (**D**) Quantification of pharyngeal pumping in N2 (wt), *tdc-1 (n3419)*, *glod-4 (gk189)*, and *tdc-1;glod-4* double mutants. (**E**, **F**) Quantification of pharyngeal pumping in N2 (wt), *tyra-2*

Figure 3 continued on next page

Figure 3 continued

(tm1846), *ser-2 (ok2103)*, *tyra-2;glod-4*, and *ser-2;glod-4* mutants. One-way analysis of variance (ANOVA) with Fisher's LSD multiple comparison test for C–F. The data points in the graphs represent the sample size (n). Comparison between two specific groups are indicated by lines above the bars; otherwise, the groups are compared with control group. *p < 0.05, **p < 0.01, ***p < 0.001, and ****p < 0.0001. Error bar ± standard deviation (SD).

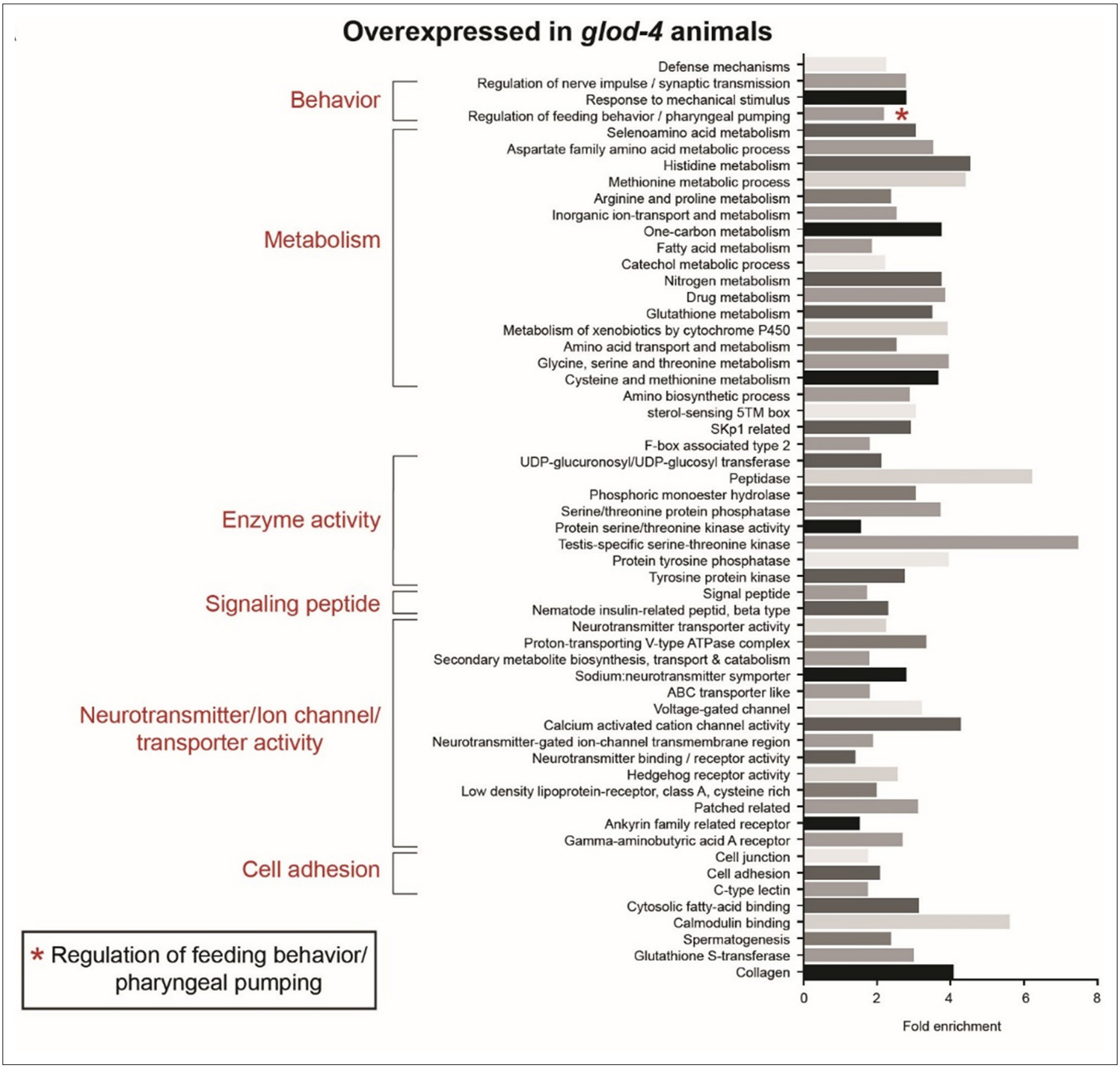

Figure 3—figure supplement 1. Gene ontology analysis for upregulated genes in *glod-4* mutant worms.

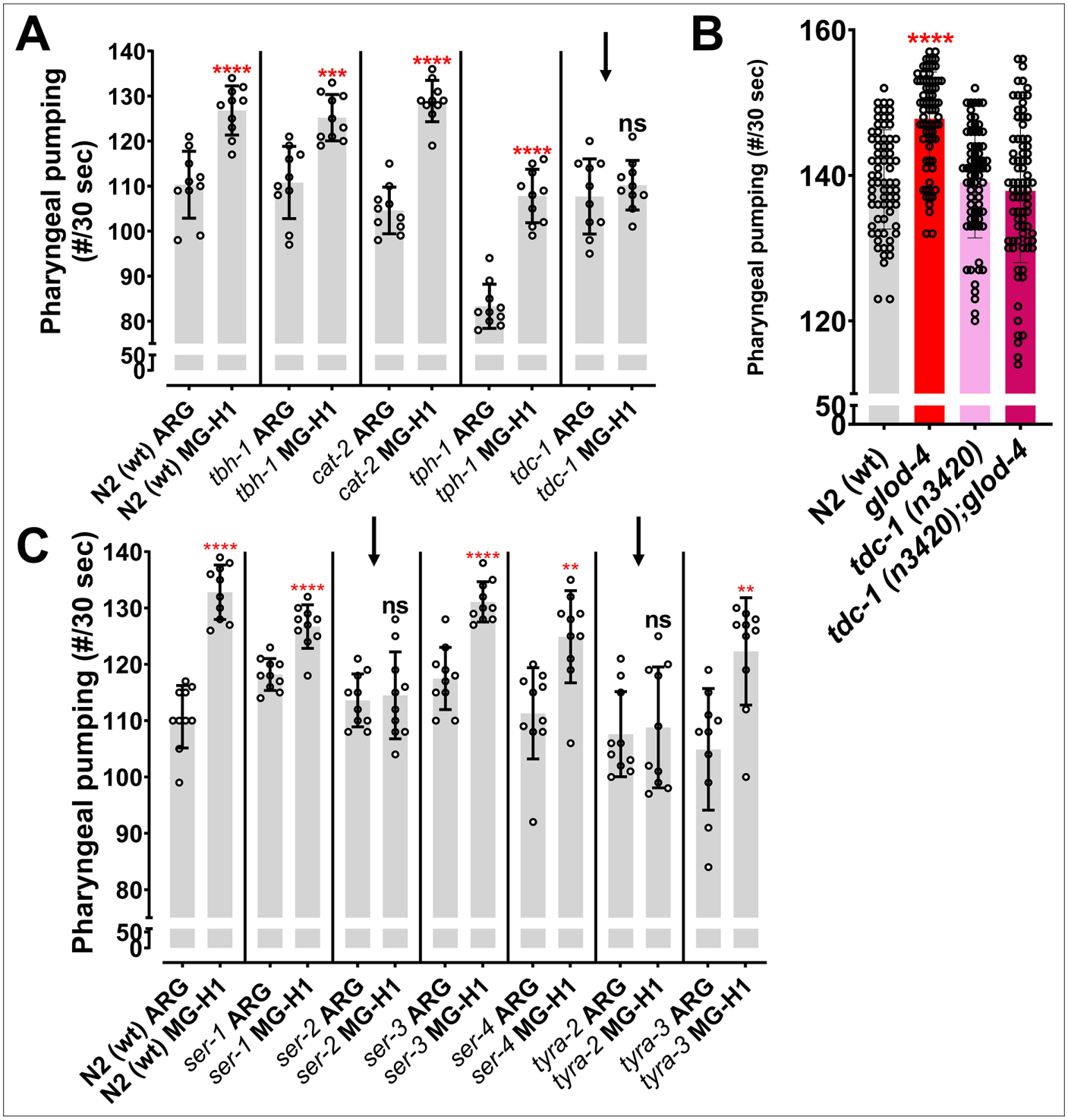

Figure 3—figure supplement 2. Role of *tdc-1* and tyramine receptors in mediating the MG-H1-induced feeding behavior. (**A**) Quantification of pharyngeal pumping (quick screening by visual counting) on mutants of enzymes involved in the biosynthesis of biogenic amines after MG-H1 treatment (suppressor screen). (**B**) Quantification of pharyngeal pumping in genetic mutants such as *tdc-1* (tyrosine decarboxylase) *n3420* allelic mutant, *glod-4* mutant, and *tdc-1;glod-4* double mutant compared with N2 wildtype worms. (**C**) Quantification of pharyngeal pumping (quick screening by visual counting) on receptor mutants involved in feeding behavior after MG-H1 treatment. Student's *t*-test for A, C. One-way analysis of variance (ANOVA) for B. The data points in the graphs represent the sample size (n). **p < 0.01, ***p < 0.001, and ****p < 0.0001. Error bar ± standard deviation (SD).

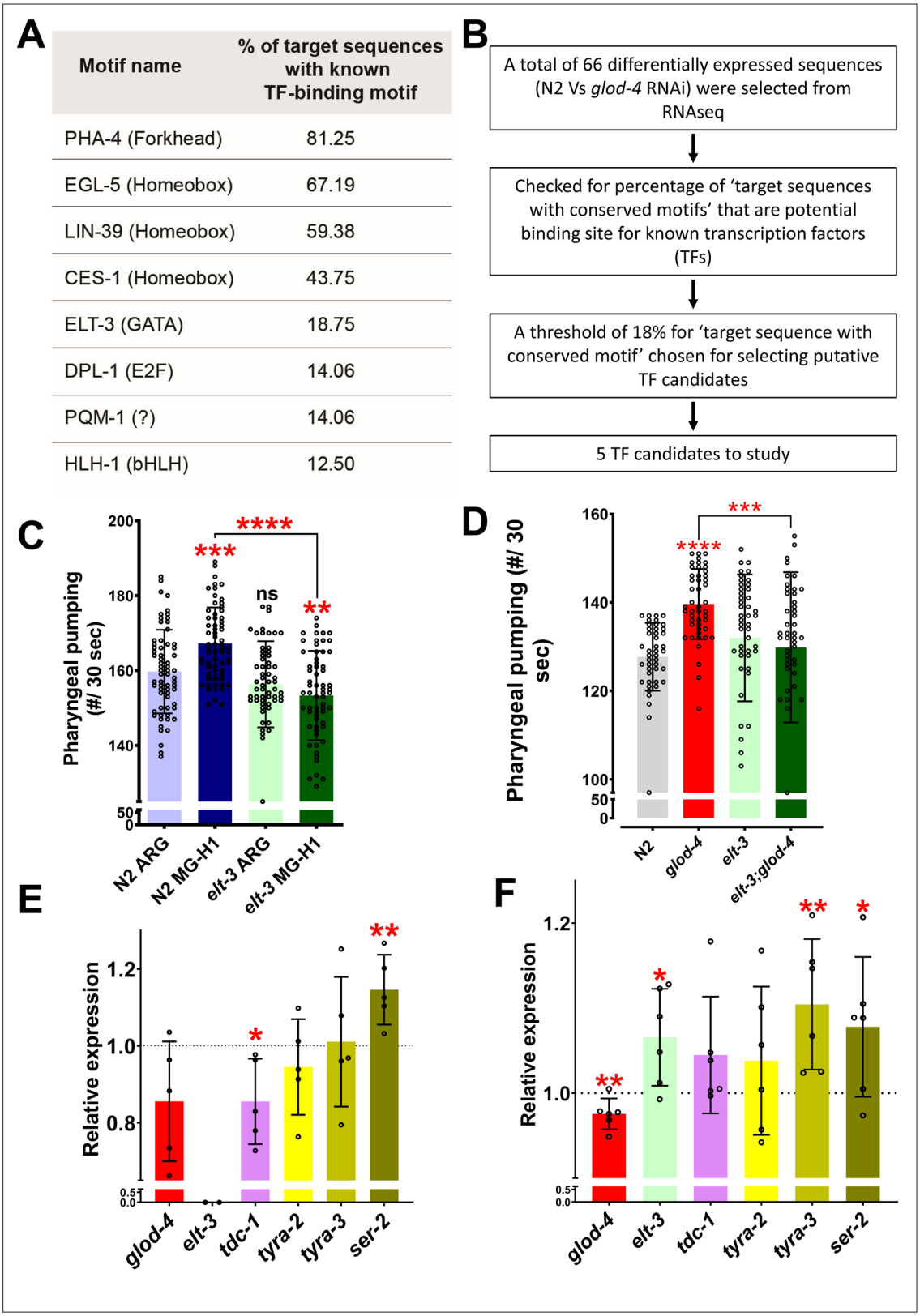

Figure 4. Role of *elt-3* transcription factor in regulating MG-H1-induced feeding in *C. elegans*. (**A**) List of transcription factors identified by motif analysis. (**B**) Flowchart demonstrating the method of identification of transcription factors. (**C**) Quantification of pharyngeal pumping after treatment with either arginine or MG-H1 in *elt-3 (gk121)* mutants. (**D**) Quantification of pharyngeal pumping in N2 (wt), *glod-4 (gk189)*, *elt-3 (gk121)*, and double mutant worms. (**E**) Quantification of tyramine pathway genes in *elt-3 (gk121)* mutant worms. (**F**) Quantification of *elt-3* and tyramine pathway genes expression in

Figure 4 continued on next page

Figure 4 continued

wildtype N2 (wt) worms after MG-H1 treatment. The horizontal dotted line indicates the normalized expression levels of genes in N2 (wt) and untreated control in E and F, respectively. One-way analysis of variance (ANOVA) with Fisher's LSD multiple comparison test for C, D. Student's *t*-test for E, F. The data points in the graphs represent the sample size (n) in C,D and number of biological repeats in E,F. Comparison between two specific groups are indicated by lines above the bars; otherwise, the groups are compared with control group. *p < 0.05, **p < 0.01, ***p < 0.001, and ****p < 0.0001. Error bars ± standard deviation (SD).

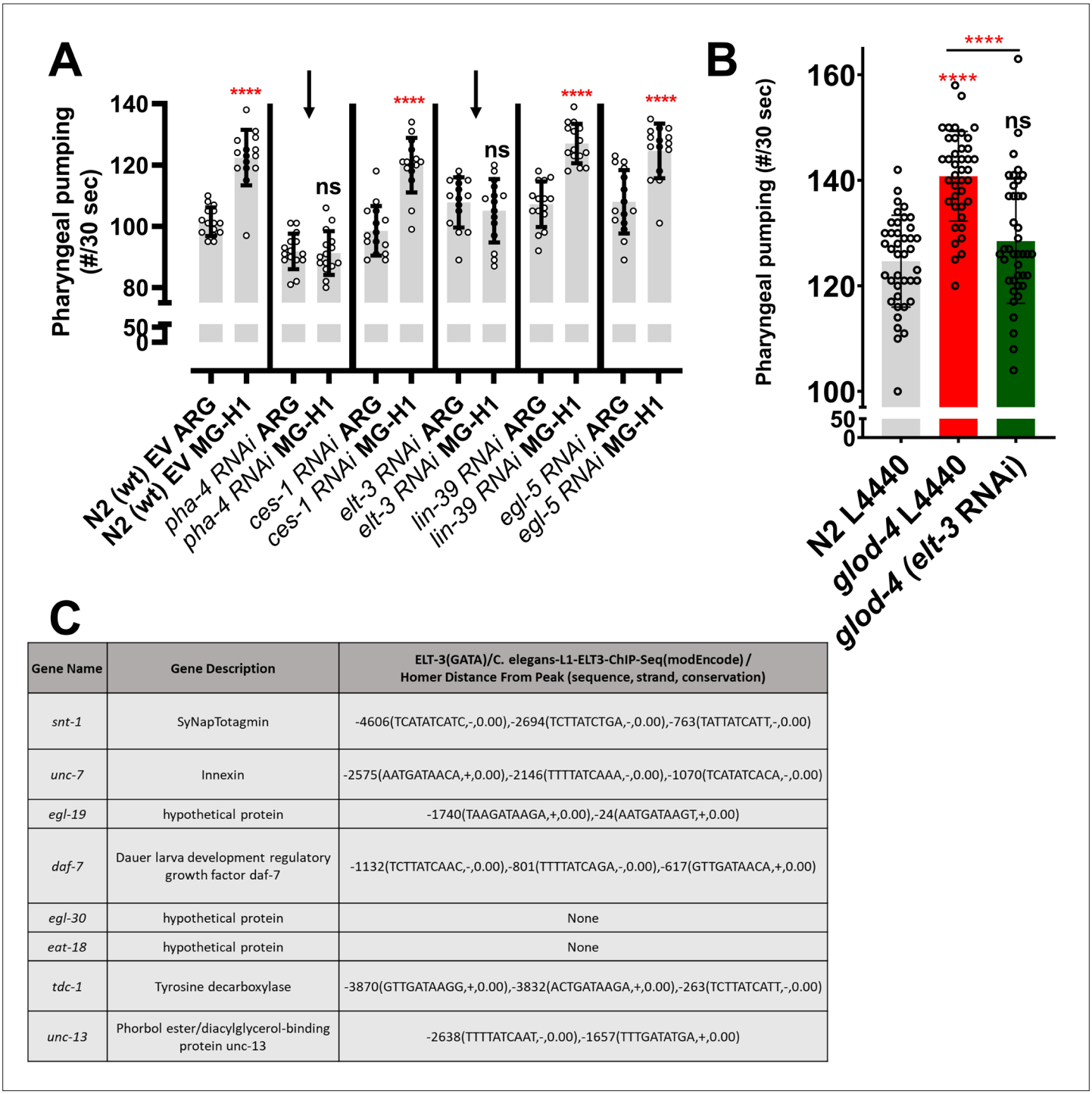

C

Gene Name	Gene Description	ELT-3(GATA)/C. elegans-L1-ELT3-ChIP-Seq(modEncode) / Homer Distance From Peak (sequence, strand, conservation)
snt-1	SyNapTotagmin	-4606(TCATATCATC,-,0.00),-2694(TCTTATCTGA,-,0.00),-763(TATTATCATT,-,0.00)
unc-7	Innexin	-2575(AATGATAACA,+,0.00),-2146(TTTTATCAAA,-,0.00),-1070(TCATATCACA,-,0.00)
egl-19	hypothetical protein	-1740(TAAGATAAGA,+,0.00),-24(AATGATAAGT,+,0.00)
daf-7	Dauer larva development regulatory growth factor daf-7	-1132(TCTTATCAAC,-,0.00),-801(TTTTATCAGA,-,0.00),-617(GTTGATAACA,+,0.00)
egl-30	hypothetical protein	None
eat-18	hypothetical protein	None
tdc-1	Tyrosine decarboxylase	-3870(GTTGATAAGG,+,0.00),-3832(ACTGATAAGA,+,0.00),-263(TCTTATCATT,-,0.00)
unc-13	Phorbol ester/diacylglycerol-binding protein unc-13	-2638(TTTTATCAAT,-,0.00),-1657(TTTGATATGA,+,0.00)

Figure 4—figure supplement 1. Role of *elt-3* transcription factor in regulating MG-H1-induced feeding in *C. elegans*. (**A**) Quantification of pharyngeal pumping (Quick visual counting), suppressor screen for top 5 transcription factors listed in ***Figure 4A***. (**B**) Quantification of pharyngeal pumping in *glod-4* mutant worms along with *elt-3* gene knockdown by RNAi feeding comparted with N2 (L4440 represent the control feeding plasmid without dsRNA). (**C**) List of genes obtained by Hypergeometric Optimization of Motif EnRichment (HOMER) analysis that are potentially regulated by the *elt-3* transcription factor. Student's *t*-test in A. One-way analysis of variance (ANOVA) for B. The data points in the graphs represent the sample size (n). ****p < 0.0001. Error bar ± standard deviation (SD).

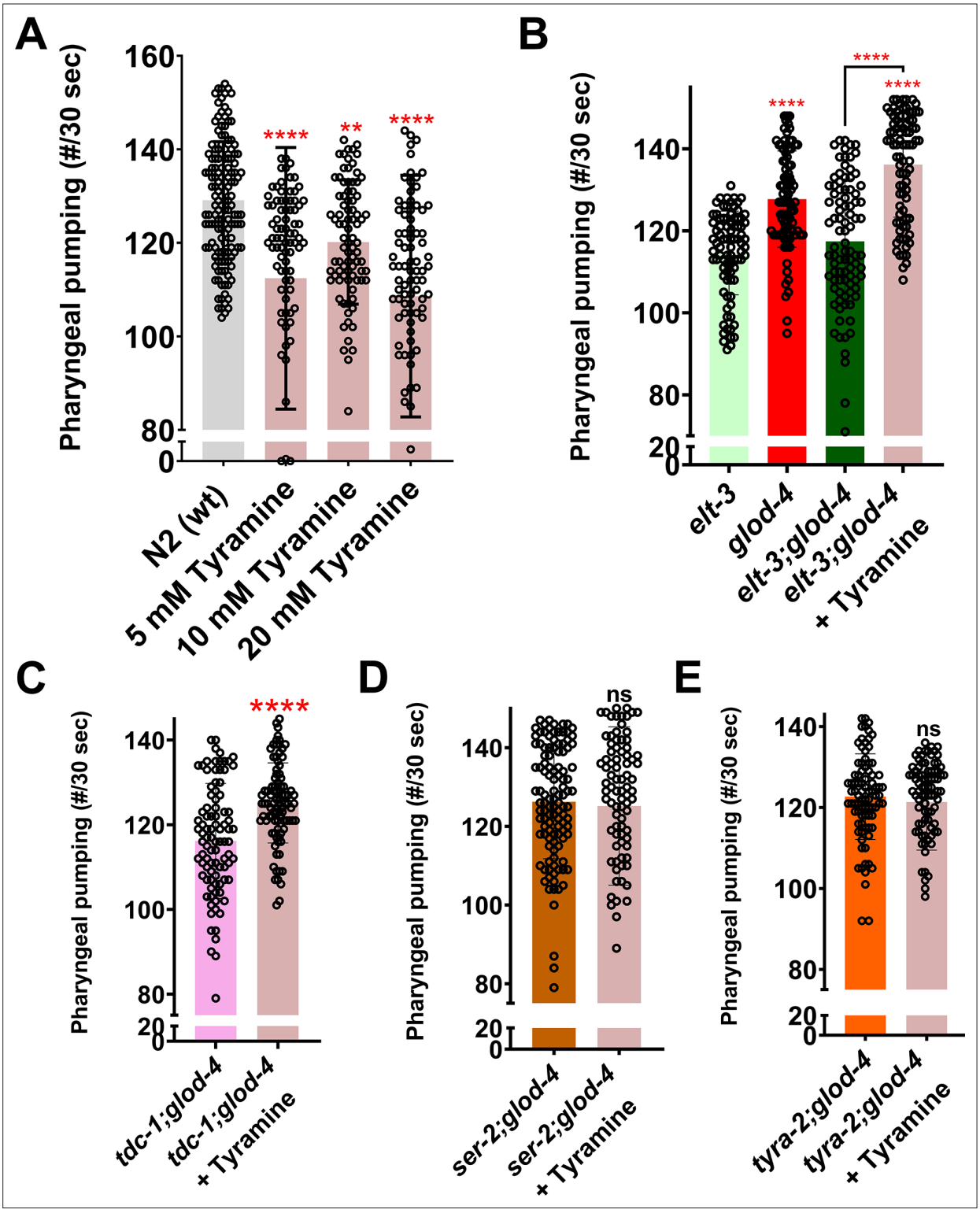

Figure 5. Exogenous tyramine rescues the suppressed pumping in double mutants. (**A**) Quantification of pharyngeal pumping in N2 wildtype worms treated with tyramine at various concentrations. (**B**) Quantification of pharyngeal pumping in *elt-3*, *glod-4*, *elt-3;glod-4* untreated and *elt-3;glod-4* double mutant treated with tyramine. (**C–E**) Quantification of pharyngeal pumping after treatment of double mutant worms (*tdc-1;glod-4*, *ser-2;glod-4*, *tyra-2;glod-4*) with exogenous tyramine. One-way analysis of variance (ANOVA) with Fisher's LSD multiple comparison test for A, B. Student's *t*-test for C–E. The data points in the graphs represent the sample size (n). Comparison between two specific groups are indicated by lines above the bars; otherwise, the groups are compared with control group. **p <0 .01, and ****p < 0.0001. Error bars ± standard deviation (SD).

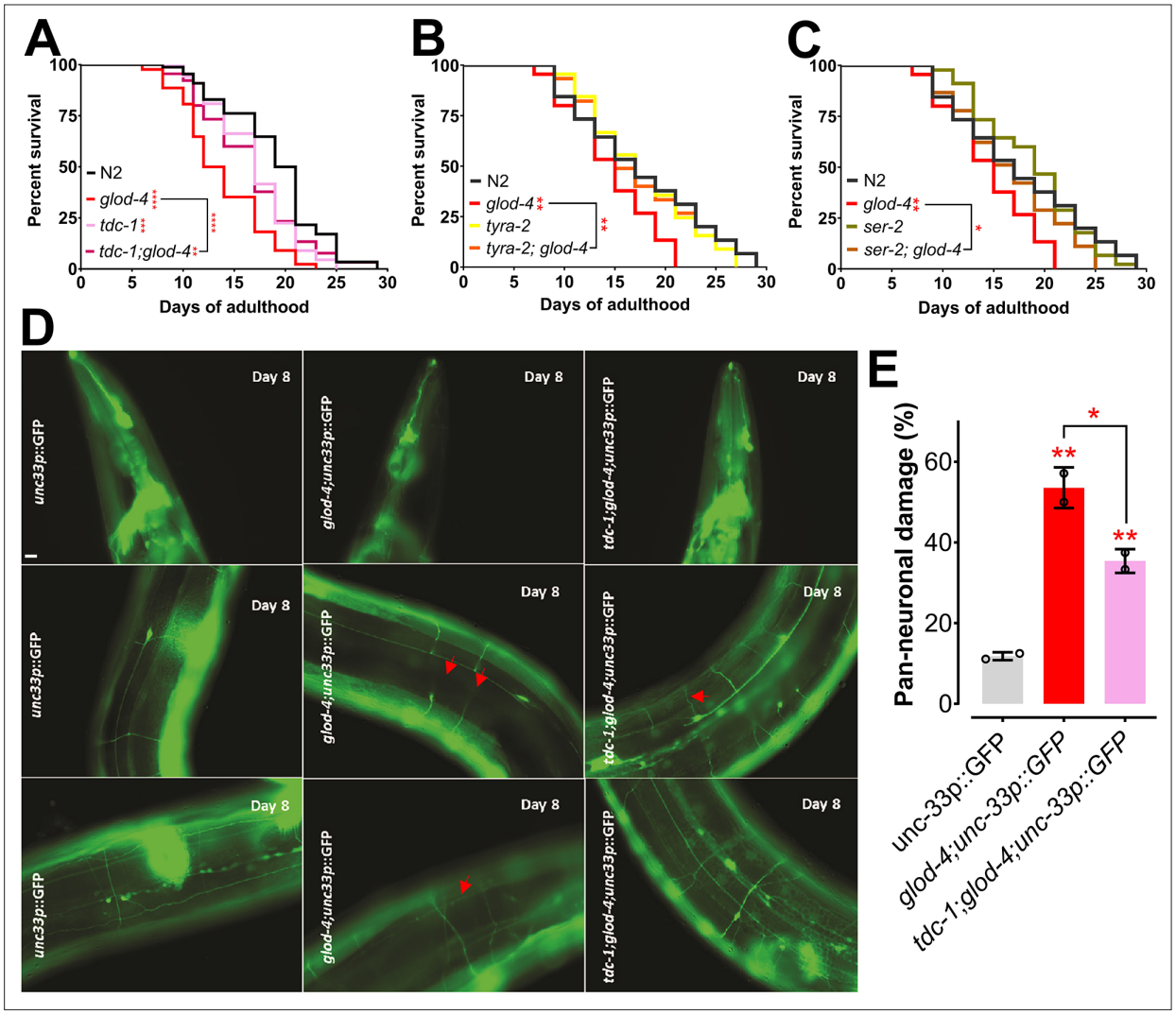

Figure 6. Suppression of *glod-4* phenotypes in *tdc-1;glod-4* double mutant. (**A**) Survival assay with N2 (wt), *tdc-1*, *glod-4*, and *tdc-1;glod-4* double mutants. (**B**) Survival assay with N2 (wt), *tyra-2*, *glod-4*, and *tyra-2;glod-4* double mutants. (**C**) Survival assay with N2 (wt), *ser-2*, *glod-4*, and *ser-2;glod-4* double mutants. (**D**) Image of worm neurons showing neuronal damage at day 8 of adulthood. Red arrows indicates damages. (**E**) Quantification of neuronal damage with pan-neuronal GFP marker in *glod-4* versus *tdc-1;glod-4* double mutants, 2 biological repeats. Scale bar – 10 μm. Log-rank (Mantel–Cox) test for survival assays. One-way analysis of variance (ANOVA) with Fisher's LSD multiple comparison test for E. Comparison between two specific groups are indicated by lines above the bars; otherwise, the groups are compared with control group. *p < 0.05, **p < 0.01, ***p < 0.001, and ****p < 0.0001. Error bar ± standard deviation (SD).

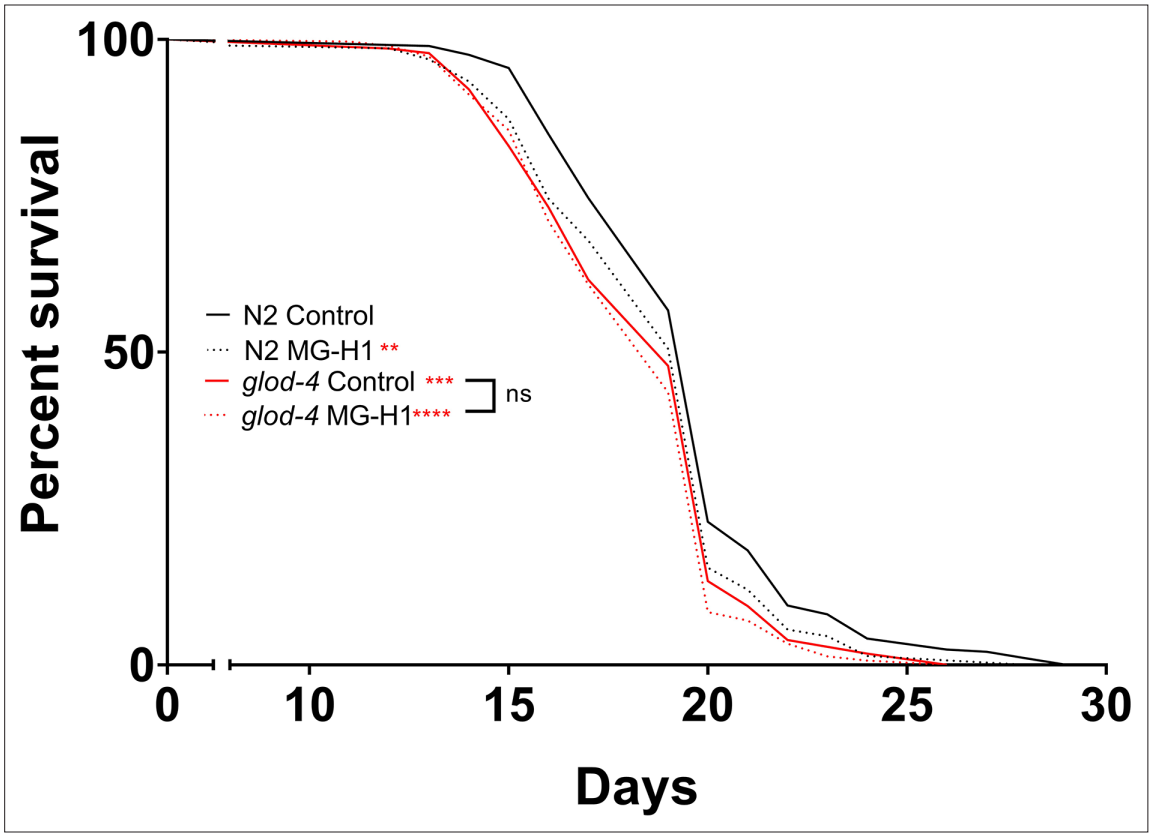

Figure 6—figure supplement 1. Survival analysis of N2 and *glod-4* mutant worms after MG-H1 treatment at 150 μM. Log-rant (Mantel–Cox) test for statistical analysis. **p < 0.01, ***p < 0.001, and ****p < 0.0001.

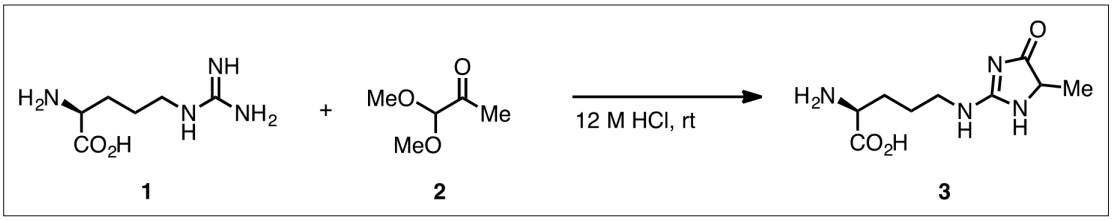

Scheme 1. Nδ-(5-hydro-5-methyl-4-imidazolon-2-yl)-ornithine (MG-H1) (3).

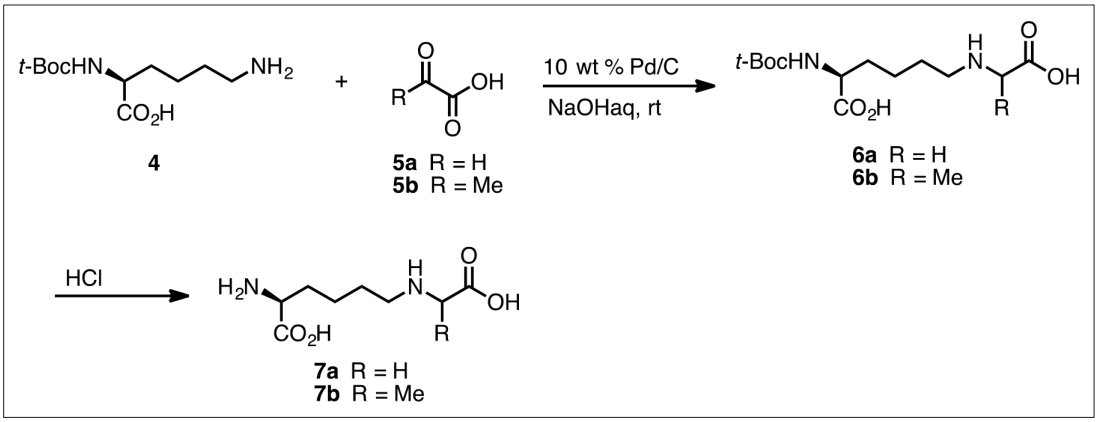

Scheme 2. Nε-carboxymethyl-lysine (CML) (7a) and Nε-(1-carboxyethyl)-lysine (CEL) (7b).

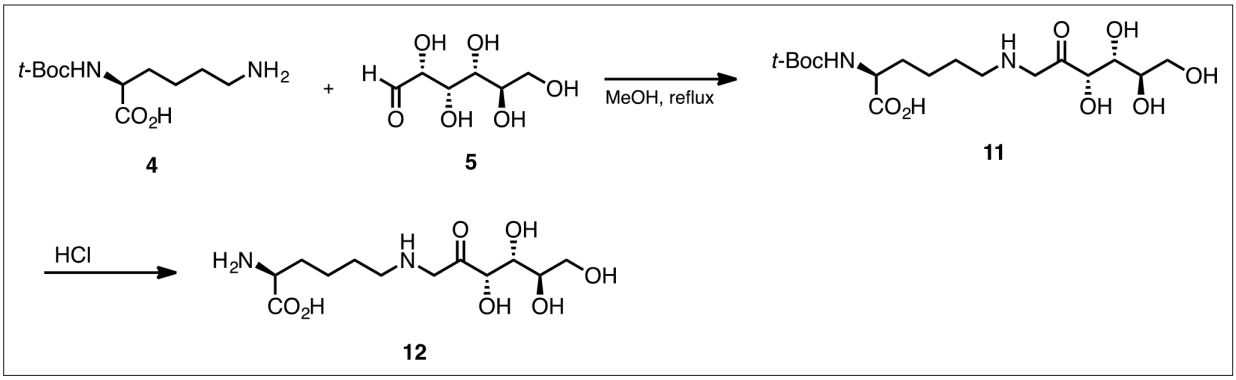

Scheme 3. Synthesis of F-ly (12).